GEOPHYSICS, VOL. 71, NO. 4 (JULY-AUGUST 2006); P. SI71–SI78, 9 FIGS., 2 TABLES.
10.1190/1.2217369

Removing free-surface multiples from teleseismic transmission and constructed reflection responses using reciprocity and the inverse scattering series

Chengliang Fan[1], Gary L. Pavlis[2], Arthur B. Weglein[3], and Bogdan G. Nita[4]

ABSTRACT

We develop a new way to remove free-surface multiples from teleseismic P- transmission and constructed reflection responses. We consider two types of teleseismic waves with the presence of the free surface: One is the recorded waves under the real transmission geometry; the other is the constructed waves under a virtual reflection geometry. The theory presented is limited to 1D plane wave acoustic media, but this approximation is reasonable for the teleseismic P-wave problem resulting from the steep emergence angle of the wavefield. Using one-way wavefield reciprocity, we show how the teleseismic reflection responses can be reconstructed from the teleseismic transmission responses. We use the inverse scattering series to remove free-surface multiples from the original transmission data and from the reconstructed reflection response. We derive an alternative algorithm for reconstructing the reflection response from the transmission data that is obtained by taking the difference between the teleseismic transmission waves before and after free-surface multiple removal. Numerical tests with 1D acoustic layered earth models demonstrate the validity of the theory we develop. Noise test shows that the algorithm can work with S/N ratio as low as 5 compared to actual data with S/N ratio from 30 to 50. Testing with elastic synthetic data indicates that the acoustic algorithm is still effective for small incidence angles of typical teleseismic wavefields.

INTRODUCTION

In reflection seismology, sources and receivers usually are located at the earth's surface (Figure 1a). In contrast, teleseismic P-wave data used in global seismology to image the deep interior of the earth utilize wavefields that are incident from below (Figure 1c). These data are collected in a transmission geometry, and the incident wavefield is well approximated by plane P-waves. Figure 1c illustrates the real teleseismic transmission geometry with a free surface. In this paper, we consider two types of teleseismic waves: One is the recorded wavefield of real teleseismic experiment under the transmission geometry (Figure 1c); the other is the constructed reflection wavefield under the virtual reflection geometry (Figure 1d). Therefore, there are two types of free-surface multiples: in the transmission geometry and in the reflection geometry, respectively.

In exploration seismology, various methods have been developed to either attenuate or eliminate free-surface multiples (Berkhout, 1982; Verschuur et al., 1992; Weglein et al., 1997; Dragoset and Jericevic, 1998). The influence of free-surface multiples on teleseismic data has been treated differently. Kennett (1991) demonstrated a way to separate P- and S-wavefield components based on polarization when the slowness and azimuth of the incident waves and the P- and S-wave velocities at the earth's surface were assumed known. In that approach, a free-surface operator was introduced to remove what is commonly called the free-surface effect. This operator, however, does nothing with multiples, but serves only to compensate for distortion of the P- and SV- particle motions from interference of upgoing and downgoing wavefields at the free surface.

In this paper, we develop a method to remove free-surface multiples from the two types of teleseismic waves. The method utilizes two different concepts. First, following Wapenaar et al. (2004), we use the one-way wavefield reciprocity theory to construct the reflection responses from transmission responses. The same relation for 1D media was derived by Claerbout (1968) in the Z-transform domain, and is the basis of acoustic daylight imaging (Rickett and Claerbout, 1999). Schuster et al. (2004) generalized the acoustic

Manuscript received by the Editor March 31, 2005; revised manuscript received January 20, 2006; published online August 17, 2006.
[1]Chevron, North America Exploration and Production, Houston, Texas 77002. E-mail: fancl@chevron.com.
[2]Indiana University, Bloomington, Department of Geological Sciences, Bloomington, Indiana 47405. E-mail: paulis@indiana.edu.
[3]University of Houston, Department of Physics, SRI-605, 617 Science and Research, Building 1, Houston, Texas 77204. E-mail: aweglein@uh.edu.
[4]Montclair State University, Department of Mathematical Sciences, 1 Normal Avenue, Montclair, New Jersey 07043. E-mail: nitab@mail.montclair.edu.

daylight imaging idea with arbitrary reflectivity and source distribution into interferometric imaging.

The second key element of the method described here is an application of the inverse scattering series (Weglein et al., 2003). The inverse scattering series is used in two different ways. First, the 1D form of the inverse scattering series for transmission geometry is used to remove free-surface multiples in the transmission wavefield. Second, the series is applied in the conventional way (seismic exploration reflection) (Weglein et al., 2003) to remove free-surface multiples in the reconstructed reflection response.

The key contribution of this paper is the unification of reciprocity theory with the inverse scattering series method to produce an approach that can remove free-surface multiples in both the transmission and reflection responses. The method has promise for major improvement estimating the impulse response of the medium with teleseismic data compared to the more conventional receiver function technique (Vinnik, 1977; Langston, 1979). Receiver functions focus on P- to S-transmission conversions. This approach has promise for estimating both the transmission and reflection responses for P-waves.

RECONSTRUCTING REFLECTION RESPONSE FROM TELESEISMIC DATA

The relationship between the reflection and transmission response has been studied by many authors for either acoustic or elastic stratified media (Claerbout, 1968; Frasier, 1970; Kennett et al., 1978; Ursin, 1983; Fokkema and Van Den Berg, 1993; Chapman, 1994; Wapenaar et al., 2004). Wapenaar and Grimbergen (1996) developed one-way (upgoing/downgoing) reciprocity theorems by using flux-normalization decomposition (see also De Hoop, 1992, 1996; Wapenaar, 1998) of the full two-way wavefield. Following Wapenaar et al. (2004), the convolution-type reciprocity theorem is

$$\int_{\Omega_1} (D_A^{\downarrow} D_B^{\uparrow} - D_A^{\uparrow} D_B^{\downarrow}) d^2\mathbf{x} = \int_{\Omega_2} (D_A^{\downarrow} D_B^{\uparrow} - D_A^{\uparrow} D_B^{\downarrow}) d^2\mathbf{x}, \tag{1}$$

and the correlation-type reciprocity theorem is

$$\int_{\Omega_1} ((D_A^{\downarrow})^* D_B^{\downarrow} - (D_A^{\uparrow})^* D_B^{\uparrow}) d^2\mathbf{x} = \int_{\Omega_2} ((D_A^{\downarrow})^* D_B^{\downarrow} - (D_A^{\uparrow})^* D_B^{\uparrow}) d^2\mathbf{x}, \tag{2}$$

where the D functions describe flux-normalized one-way wavefields. The superscript arrows stand for upgoing and downgoing components and the subscripts A and B represent two independent acoustic seismic experiments (Figure 2). The superscript * means complex conjugate of the wavefield components, and Ω_1 and Ω_2 are horizontal integration boundaries. In our case, we assume Ω_1 is just below the free surface and Ω_2 is the bottom surface of the medium. The correlation-type reciprocity, which is used in this paper, assumes that the wavefields have no evanescent components and the medium between Ω_1 and Ω_2 is lossless and source free.

Because downgoing and upgoing one-way wavefields are related directly to the reflection and transmission response (see Wapenaar et al. (2004) for more details), the reciprocity relations for the one-way wavefield (equations 1 and 2) provide useful relationships between these wavefield components. Source-receiver reciprocity relations can be obtained by considering different pairs of acoustic seismic experiments using the convolution-type reciprocity relation defined by equation 1. When A and B are two acoustic seismic-reflection experiments, we can obtain source-receiver reciprocity for the reflection responses just above Ω_1 on the free surface as

$$R_r^{fs}(\mathbf{x}_A, \mathbf{x}_B, \omega) = R_r^{fs}(\mathbf{x}_B, \mathbf{x}_A, \omega). \tag{3}$$

Each side of the above equation represents the reflection response with a free surface of one independent seismic reflection experiment. The reflection response, in general, is a function of source position, receiver position, and angular frequency. Subscript r stands

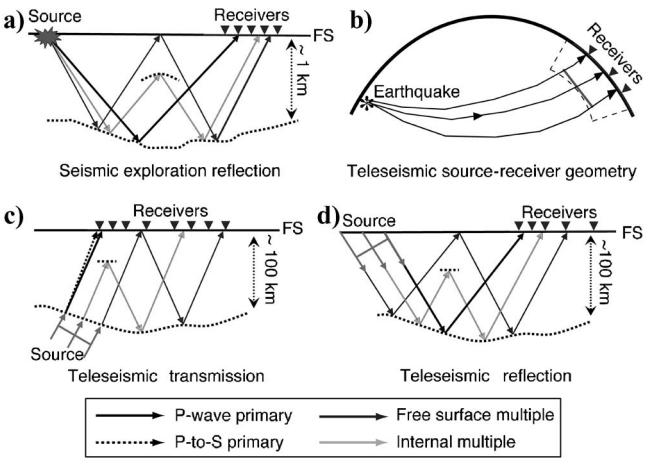

Figure 1. Illustration of teleseismic and seismic exploration geometries. Primaries and multiples are indicated by solid (P-waves) and dashed (S-waves) arrows. (a) Illustration of seismic exploration reflection geometry. A point source and regularly spaced receivers are located at the free surface (FS). The main waves include reflection primary, free surface, and internal multiples. (b) Illustration of the overall teleseismic geometry. The actual source (earthquake) is located at a large distance (30°–90°) from the receiver array, and the incident wavefield can be assumed to be well approximated by a plane wave. (c) Definition of teleseismic transmission geometry. We have a plane P-wave source field incident from below and irregularly spaced receivers at the free surface. The main waves are transmitted P-waves, P-to-S conversions, free-surface multiples and internal scatterings. (d) Definition of the teleseismic virtual reflection geometry. A virtual P-wave source and irregularly spaced receivers are at the free surface. All teleseismic reflection waves are constructed from the teleseismic transmission waves defined by (c). The main-wave components are reflection primary, free surface, and internal multiples.

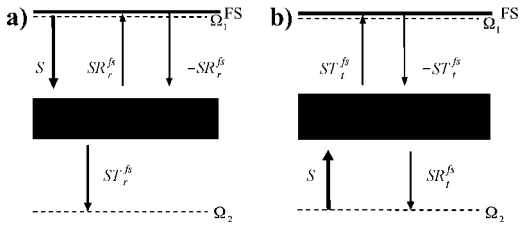

Figure 2. Reflection (a) and transmission/teleseismic (b) experiments in 3D inhomogeneous source-free media between two boundaries with the top boundary (a free surface). In this figure, S is the source wavelet; R and T are reflection and transmission responses; subscript r and t stand for reflection and transmission geometry, and superscript fs indicates responses with free-surface multiples.

for reflection geometry, and the superscript *fs* indicates reflection response with a free surface present. Relationship 3 shows that the source and receiver positions can be interchanged on the free surface.

For the teleseismic problem, we need to assume that A and B are independent seismic experiments with different geometries illustrated in Figure 2. That is, we assume one is the reflection geometry and the other is the transmission geometry. The source-receiver reciprocity relation for the transmission responses at Ω_1 and Ω_2 is

$$T_r^{fs}(\mathbf{x}_A,\mathbf{x}_B,\omega) = T_t^{fs}(\mathbf{x}_B,\mathbf{x}_A,\omega), \tag{4}$$

where the subscript t stands for transmission geometry (Figure 2). Following Wapenaar et al. (2004), if we consider A and B as independent, acoustic, seismic reflection experiments, the correlation-type reciprocity relation, equation 2, requires

$$\delta(\mathbf{x}_{BH}-\mathbf{x}_{AH}) - R_r^{fs}(\mathbf{x}_A,\mathbf{x}_B,\omega) - (R_r^{fs}(\mathbf{x}_B,\mathbf{x}_A,\omega))^* = \int_{\Omega_2} (T_r^{fs}(\mathbf{x},\mathbf{x}_A,\omega))^* T_r^{fs}(\mathbf{x},\mathbf{x}_B,\omega)\mathrm{d}^2\mathbf{x}, \tag{5}$$

where the subscripts $\mathbf{x}_{BH}$ and $\mathbf{x}_{AH}$ emphasize that the spatial variables ($\mathbf{x}_B$ and $\mathbf{x}_A$) are constrained to earth's surface. Combining equation 5 with the source-receiver reciprocity relations (equation 3 and 4), we obtain

$$2\,\mathrm{Re}[R_r^{fs}(\mathbf{x}_A,\mathbf{x}_B,\omega)] = \delta(\mathbf{x}_{BH}-\mathbf{x}_{AH}) - \int_{\Omega_2} (T_t^{fs}(\mathbf{x}_A,\mathbf{x},\omega))^* T_t^{fs}(\mathbf{x}_B,\mathbf{x},\omega)\mathrm{d}^2\mathbf{x}, \tag{6}$$

where $\mathrm{Re}[\bullet]$ means the real part of the complex spectrum. The above equation shows that the real part of the reflection response with the conventional reflection experiment can be constructed from the transmission response of a distribution of sources below. Because the impulse response of P-waves in the reflection experiments is causal in the time domain, the imaginary part can be obtained by taking the Hilbert transform of the corresponding real part (Claerbout, 1976; Karl, 1989; Wapenaar et al., 2004). For plane waves in 1D acoustic media, the relation between the reflection and transmission response is

$$2\,\mathrm{Re}[R_r^{fs}(\omega)] = 1 - (T_t^{fs}(\omega))^* T_t^{fs}(\omega). \tag{7}$$

The above theory was derived by Wapenaar (2003) using power conservation and tested with synthetics by Wapenaar et al. (2003). The same relation was derived by Claerbout (1968) in the Z-transform domain, which is the basis of acoustic daylight imaging (Rickett and Claerbout, 1999). Schuster et al. (2004) generalized the acoustic daylight imaging idea with arbitrary reflectivity and source distribution into interferometric imaging. In this paper, we will use the relation between the reflection and transmission response (equation 7) to obtain the constructed reflection. This will allow us to apply the inverse scattering series to the teleseismic transmission geometry to remove free-surface multiples.

FREE-SURFACE MULTIPLE REMOVAL FROM THE TELESEISMIC WAVEFIELD

The inverse scattering series has been used to eliminate free-surface multiples in reflection seismic exploration (Weglein et al., 1997). Here we show that for the teleseismic experiment, free-surface multiples can be removed from the total recorded teleseismic wavefield. The free-surface multiples are particularly strong with the normal or close-to-normal incidence that characterizes the teleseismic P-wave problem. In general, large aperture broadband arrays undoubtedly record strong free-surface reverberations. Most existing methods, however, are incapable of any separation of the total teleseismic wavefield. The only exception is the principle component method Bostock and Rondenay (1999) used to approximately separate direct and scattered waves. That method, however, is based on an assumption that the free-surface reflected wavefield is random when averaged across the entire array.

A series relationship between the reflection responses with and without a free surface can be obtained for a 1D acoustic medium for the geometry shown in Figure 3. We initially assume an incident downgoing plane wave. Because the free surface has a reflection coefficient of -1, Weglein et al., (2003) show that

$$R_r^{fs}(\omega) = R_r(\omega)(1 - R_r(\omega) + (R_r(\omega))^2 - (R_r(\omega))^3 + \cdots) = R_r(\omega)/(1 + R_r(\omega)). \tag{8}$$

Rewriting the above equation, we can get the impulse response of the reflection experiment without free-surface multiples as a series in terms of the reflection response with free-surface multiples

$$R_r(\omega) = R_r^{fs}(\omega)/(1 - R_r^{fs}(\omega)) = R_r^{fs}(\omega) + (R_r^{fs}(\omega))^2 + (R_r^{fs}(\omega))^3 + \cdots. \tag{9}$$

For the teleseismic transmission problem, again assuming a 1D acoustic medium we can obtain a similar relationship between the transmission and reflection response (Figure 4). Let the transmission response without a free surface (Figure 4a) be $T_t(\omega)$, and the transmission response with a free surface present (Figure 4b) be $T_t^{fs}(\omega)$. The relation of these two transmission response functions is shown by Figure 4c. That is,

$$T_t^{fs}(\omega) = T_t(\omega)(1 - R_r(\omega) + (R_r(\omega))^2 - (R_r(\omega))^3 + \cdots) = T_t(\omega)/(1 + R_r(\omega)). \tag{10}$$

Hence, using the same series form as equation 9, the transmission response without free-surface multiples can be obtained by

$$T_t(\omega) = T_t^{fs}(\omega)/(1 - R_r^{fs}(\omega)) = T_t^{fs}(\omega)(1 + R_r^{fs}(\omega) + (R_r^{fs}(\omega))^2 + \cdots), \tag{11}$$

where $R_r^{fs}(\omega)$ is the reflection response of the media with the free surface present. Equation 11 is the most important result of this paper.

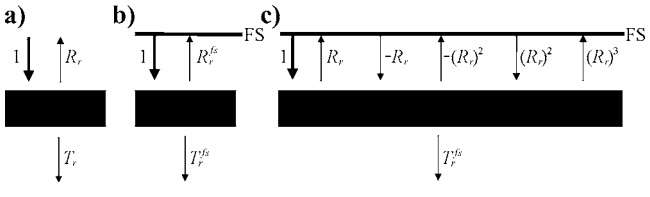

Figure 3. Enumeration of wavefield components in a reflection experiment for 1D acoustic earth with unit-amplitude normal-incidence source wavefield, with and without a free surface. (a) Seismic reflection without a free surface; (b) seismic reflection with a free surface; (c) free-surface multiples of seismic reflection experiment. The symbols are defined as in Figure 2.

The key idea is that $R_r^{fs}(\omega)$ can be reconstructed from $T_t^{fs}(\omega)$ by equation 7. $T_t^{fs}(\omega)$ is related to the recorded teleseismic data $D(\omega)$ by

$$D(\omega) = S(\omega)T_t^{fs}(\omega), \tag{12}$$

where $S(\omega)$ is a source wavelet. Estimating the source signature is a fundamental problem in handling real teleseismic P-wave data (e.g. Baig et al., 2005, or Pavlis, 2003, 2005). For the present, we will assume $S(\omega)$ known and we can obtain $T_t^{fs}(\omega)$ from $D(\omega)$ through some form of deconvolution. In the discussion section, we consider this limitation further. Equation 11 is still very important because it provides a new way to remove free-surface multiples from the teleseismic transmission P-wave response function.

RECONSTRUCTING THE REFLECTION RESPONSE FROM TELESEISMIC FREE-SURFACE MULTIPLES

After free-surface multiples are removed from the total teleseismic transmission wavefield, the remaining wavefield contains pure transmission waves and internal scatterings from the lithosphere or the upper mantle. We can exploit this insight and take the difference

$$T_t^{fsm}(\omega) = T_t^{fs}(\omega) - T_t(\omega), \tag{13}$$

where $T_t^{fsm}(\omega)$ are the pure free-surface multiples in the transmission response. The internal multiples are also canceled on the right side of equation 13 in $T_t^{fs}(\omega)$ and $T_t(\omega)$ by the subtraction.

For the acoustic approximation assumed here, equation 13 is related closely to the reflection response. In particular, for the teleseismic plane waves, we can reconstruct the reflection response as

$$R_r^{fs}(\omega) = -QT_t^{fsm}(\omega)e^{i\omega t_T}, \tag{14}$$

where Q is a constant representing an overall amplitude difference and t_T is the travel-time delay of pure transmission waves through the study region. Equation 14 says that $T_t^{fsm}(\omega)$ is the same as the reflection response except for an amplitude factor and a completely predictable time shift. $R_r^{fs}(\omega)$ and $T_t^{fsm}(\omega)$ have opposite signs because of the -1 free-surface reflection coefficient. In fact, substituting equation 11 into equation 13 produces

$$R_r^{fs}(\omega) = -T_t^{fsm}(\omega)/T_t(\omega). \tag{15}$$

Equation 15 is an approximation of equation 14 when the internal multiples in the transmission response are ignored. Once the free-surface multiple removal in $T_t^{fs}(\omega)$ is complete, $R_r^{fs}(\omega)$ obtained by equation 14 is close to that constructed by equation 7. Equation 14 provides an important, fundamental insight: Both the constructed reflection waves — from the virtual reflection geometry and the waves generated by the transmission wavefield acting as a secondary source at the free surface — can be used as an indication of the impulse response of the earth.

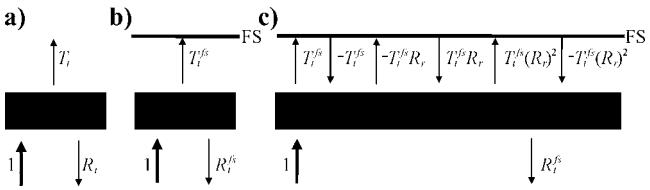

Figure 4. Enumeration of wavefield components in a transmission experiment (teleseismic geometry) for a 1D acoustic earth with unit-amplitude normal-incidence source wavefield, with and without a free surface. (a) Transmission without a free surface; (b) transmission with a free surface; (c) free surface reverberations. The symbols are defined as in Figure 2.

SYNTHETIC EXAMPLES

Synthetic tests for 1D acoustic model

We generated synthetic data sets to test the above concepts by convolving a computed impulse responses with a source wavelet (e.g., Figure 5). The synthetics were generated using the $\tau - p$ method with a 1D acoustic medium (Table 1) using a package developed by Herrmann (2002). Figure 5 was produced by convolving the computed impulse response (slowness of 0.12 s/km) with a simulated source wavelet that was produced from actual teleseismic P-wave signals. The simulations model a range of ray parameters, from 0 to 0.12 s/km, consistent with actual teleseismic P-waves. The free surface causes free-surface multiples seen in Figure 6a that are effectively removed by application of equation 11. The transmission response with free-surface multiples removed is a pure delta function pulse except for a small internal multiple response (e.g., about 12 s after the direct wave for slowness of 0 in Figure 6a).

The constructed reflection response (Figure 6b) is identical to the reflection impulse response corresponding to the three-layer model. Figure 6b also shows how the conventional reflection series removes free-surface multiples. This demonstrates the benefit of using this approach to recover primary reflections from the lower crust to upper mantle.

Figure 6c validates the separation concept of equation 13 and also confirms the results of the construction procedure of reflection re-

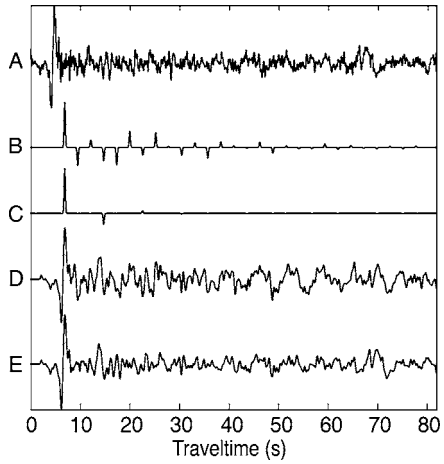

Figure 5. Illustration of synthetic source wavelet, teleseismic responses and data with/without free-surface multiples. Trace A is a source wavefield used to simulate real data. It is an actual teleseismic P-wave. Trace B is the teleseismic impulse response of a three-layer lithospheric acoustic earth model with the free surface; trace C is the teleseismic response after free-surface multiple removal. The remaining pulses correspond to the transmission primary and internal multiples. Trace D is the simulated teleseismic data with the free-surface multiples. It is generated by the convolution of A and B. Trace E is simulated teleseismic data after free-surface multiple removal. D and E illustrate that the data before and after free-surface multiple removal do not look very different. This is a common property of real teleseismic data in which the source wavefield has a long duration compared to the impulse response of interest.

sponses (dashed traces in Figure 6b) using equation 7. It works also because the internal multiples in the transmission response in equation 14 are canceled by the subtraction.

We also experimented with an eight-layer acoustic model (Table 2) to understand how the method might respond with a significant transmission energy delayed by internal multiples (Figure 7). It shows that when an earth model has more variability, the theory is equally valid, and we can still segment primary transmitted P, primary reflected P, and multiples. The transmitted wavefield estimate contains some residual energy from internal multiples, but the transmitted pulse is a much closer approximation to the desired delta function. It also shows that when the earth model becomes more complex, more multiples are present and free-surface multiple removal becomes more significant.

Tests for synthetic noise data

All the above synthetic results were produced under the assumption of an ideal case with no noise. However, all real teleseismic data have different levels of natural noise. To test the sensitivity of the algorithm to noise, we produced a set of simulated noisy data from the three-layer acoustic model (Table 1) at different S/N ratios. The S/N ratios are defined here as the ratios of peak amplitudes of the signal and noise. The simulated noisy data (Figure 8a) were produced by adding varying levels of Gaussian white noise to synthetics convolved with a simulated teleseismic source wavelet (Figure 5). Here we are assuming that the source wavelet is known accurately. We estimated the impulse response of the noisy, simulated data by estimating an inverse wavelet using a convolutional quelling operator (Backus, 1970; Meyerholtz et al., 1989) with a Gaussian smoothing filter (e.g., Lindenbaum et al., 1994) with a pulse width of 1 s (Figure 8b). This method is useful for this application because teleseismic data are always band-limited at high frequencies, but less limited at low frequencies. The results are shown in Figure 8c. It is clear that with an S/N ratio higher than 5, the constructed reflection responses are acceptable and the free-surface multiple removal techniques are effective (Figure 8). It is important to note that SNR of real data is usually much higher than 5. When we constructed the impulse response using a devonvolution operator constructed from the (assumed known) wavelet, the noise in the impulse response was strongly suppressed. This occurs for the same reason that vibroseis works. The white noise we added has an autocorrelation equal, in the limit, to a delta function. Convolution with the inverse operator derived from the source wavelet reduces the noise by using a weighted average over the length of the inverse operator. This is encouraging because it says that if we can estimate the source wavelet accurately, we can potentially utilize data at modest S/N ratios. Estimating the source wavelet is, however, potentially problematic. We discuss this further in the Discussion section.

Table 1. Three-layer lithospheric earth model.

Layer lower boundary depth (km)	P-wave velocity (km/s)	S-wave velocity (km/s)	Density (g/cm^3)
6	4	2.3	2.3
40	6	3.5	2.8
>40	8	4.7	3.3

ACOUSTIC THEORY APPLIED TO ELASTIC DATA

The theory described above is for 1D acoustic media but could potentially be expanded to an elastic multidimension version (Weglein

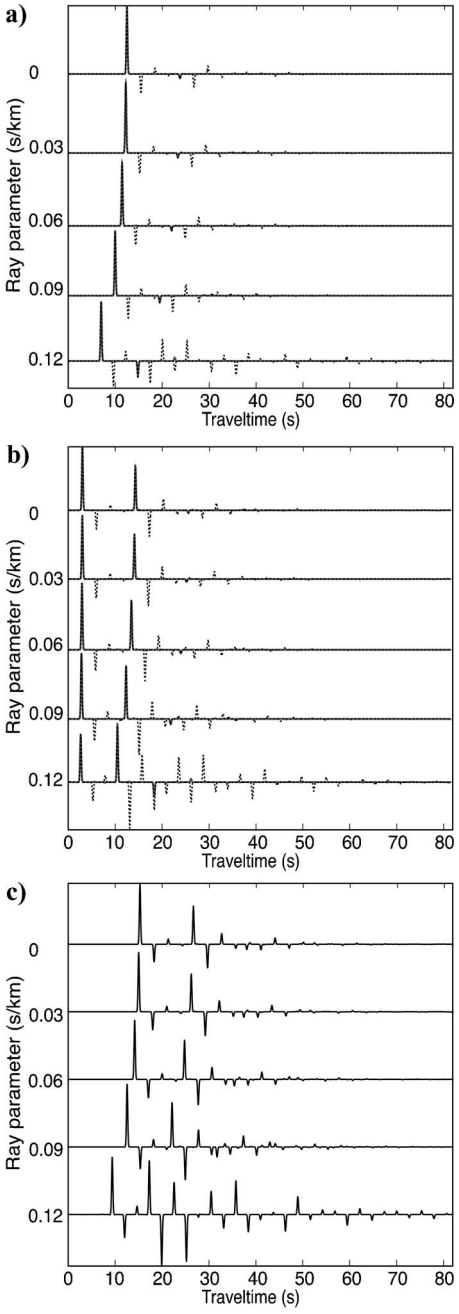

Figure 6. For a three-layer lithospheric earth model with different ray parameters, (a) teleseismic responses before (dashed) and after (solid) free-surface effect removal and (b) reflection responses are reconstructed using equation 7. In both (a) and (b), the original response is shown as a dashed curve, and the result after free-surface multiple removal is shown as a solid curve. Note that in this and similar figures that follow, the solid curves often totally cover up the dashed curves because the primaries are not altered by the free-surface multiple-removal procedure. (c) Impulse response of free-surface multiples separated from (a) using equation 13 and multiplied by −1 (solid curve), compared to the reconstructed reflection responses in (b) (dashed traces), computed using equation 7.

et al., 2003; Wapenaar et al., 2004). The main contribution of this paper is that it is the first to unify the concepts of the reflection/transmission reconstruction at a free surface with the inverse scattering series. The extensions to elastic and 3D media will require additional work. Nonetheless, we note that additional synthetic elastic experiments demonstrate that an acoustic assumption is probably better than one might guess.

We tested the above 1D acoustic theory with a three-layer, elastic wave model (Table 1). The incident wave slowness values range from 0 (vertical incidence) to 0.12 s/km (a phase velocity of 8.3 km/s). In examining these results, note that it is currently routine practice to use only teleseismic P-wave data in a distance range of 30° to 90° (or about 3330 to 9990 km, corresponding to slowness of 0.042 and 0.079 s/km, respectively). The reasons for this are pragmatic: Real data from sources at distances less than 30° are complicated by triplications caused by upper mantle discontinuities, and data from sources at distances greater than 90 degrees are complicated by interaction with the core-mantle boundary. Hence, only the 0.06 s/km simulation is within the range of current data-processing practice. We present a wider range of results, however, as the full suite is useful to appraise the validity of the acoustic approximation.

Table 2. Eight-layer acoustic lithospheric earth model.

Layer lower boundary depth (km)	P-wave velocity (km/s)	Density (g/cm^3)
2	2.8	2.0
8	4.0	2.4
12	3.0	2.1
20	4.8	2.6
30	5.5	2.8
40	6.3	3.0
60	8.8	3.8
>60	7.0	3.3

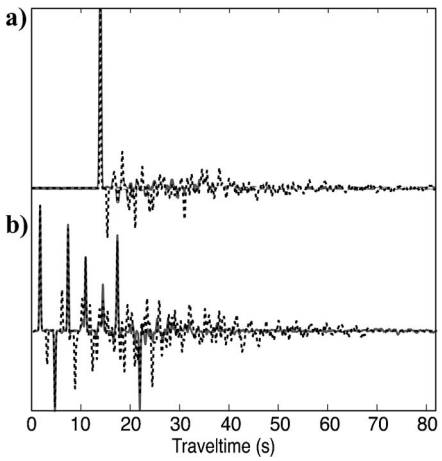

Figure 7. (a) Teleseismic response from normal-incident plane P-waves of an eight-layer lithospheric earth model before (dashed) and after (solid) free-surface multiple removal, (b) reconstructed reflection responses from normal-incident plane P-waves of an eight-layer acoustic lithospheric earth model before (dashed) and after (solid) free-surface multiple removal.

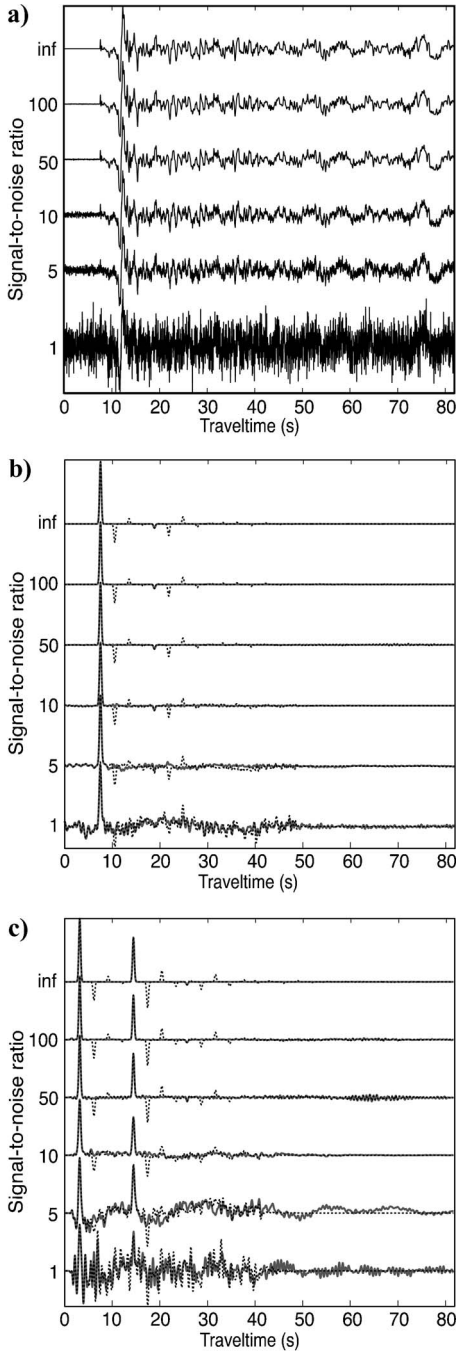

Figure 8. Noisy data simulation results. (a) Teleseismic data with different level of white noise and (b) the transmitted wave impulse response computed from (a) using a deconvolution filter constructed from the actual source wavelet used to generate the simulated data. The dashed line is the impulse response before free-surface multiple removal, and the solid line is the impulse response with free-surface multiples removed. Compared to (b), (c) shows the reconstructed reflection responses for varying S/N ratios. We note that in lower S/N conditions, the process of removing free-surface multiples from the teleseismic transmission data using the transmission series expansion (where the reconstructed reflection is used) delivers better results compared to the results from only reconstructing the reflection response, because of the dominant amplitude of the first arrival in transmission response. The reconstructed reflection response corresponds to a three-layer acoustic lithospheric earth model before (dashed) and after (solid) free-surface multiple removal.

One should keep in mind that for this model and this set of incident slowness vectors, increasing slowness always leads to increasingly strong P-to-S conversions. Hence, the acoustic approximation becomes progressively poorer as slowness increases.

We would argue that the results of this set of simulations show two things worth noting.

First, the acoustic approximation is less of a problem for removing free-surface multiples from the transmission response than it is for constructing the reflection response. Figure 9a shows that our method, based on the acoustic approximation, reduces the transmission response to a fair approximation of the direct P impulse even for unrealistically low phase velocities. This is not true for the constructed reflection response (Figure 9b). The reflection response is increasingly impacted by S-to-P conversions as slowness increases. The resulting multiples are, as expected, eliminated by the acoustic multiple-removal method with two types of primaries remained: P reflected and S-to-P converted primaries. For both transmission and reflection responses, the free-surface multiples (including both reflected and converted P-waves) are predicted correctly and removed. This is because the inverse scattering series method works for (P, S) component data (Weglein et al., 2003).

Second, exploiting polarization helps very little in this case. Figures 9c and d show the effect of using Kennett's (1991) free-surface transformation matrix (p subscript) compared to using data from a simple vertical component instrument (z subscript). Because of the near-vertical incidence of the wavefield in this geometry, polarization does not have a large effect. Furthermore, Figure 9d shows that the mixed mode primary reflections (events B′ and D′ in Figure 9d) are the largest noise pulses in this reconstructed reflection response. The polarization transform cannot eliminate this type of mixed-mode path because it is recorded as an upgoing P-wave, after one leg as a downgoing S-wave. Clearly, a full elastic theory is needed to separate this type of wave component from the full wavefield.

DISCUSSION

This paper is in a special section devoted to interferometric/daylight imaging. It is worthwhile discussing why this paper has any relevance to that problem at all. The main answer is that daylight imaging with P-waves commonly appeals to the reciprocity relations we described above and applies them as the theoretical basis for reconstructing the equivalent reflection response using crosscorrelation of the noise field. In daylight imaging, a critical assumption is that the noise field is being generated by randomly distributed sources so that ensemble averages are not biased by spatial coloring of the noise field. The theory we describe here is linked to daylight imaging by the transmission-to-reflection transformation operator. The way we expect to use it, however, is totally different. The expected primary application of this technique is to improve methods for imaging the earth with teleseismic body waves.

The potential application of this approach to real teleseismic data has two elements. The first is the estimation of the P-to-SV transmission conversion strength commonly called *receiver functions* (Vinnik, 1977; Langston, 1979; Pavlis (2003, 2005), have argued that the conventional methods for computing receiver functions are founded on an assumption that is demonstrably wrong in ways seen in synthetics in this paper. That is, the conventional approach assumes that the vertical component data are the source wavelet. As this paper demonstrates, the data recorded at the surface are not the source wavelet, but the source wavelet altered by the transmission response of the medium with the free surface present. Our simulations show that removing free-surface multiple components from the transmitted wavefield leads to an impulse response that is a very good approximation to a single impulse at the arrival time of the direct (ballistic) wave. With this insight, a potential wavelet estimation scheme is similar to that used in reflection multiple removals methods using the inverse-scattering series (Matson, 2000). The basic idea is to invert for the wavelet by finding one that minimizes the output energy in the reconstructed reflection response with multiples removed (equation 9). This wavelet potentially can provide a more accurate representation of the source wavelet

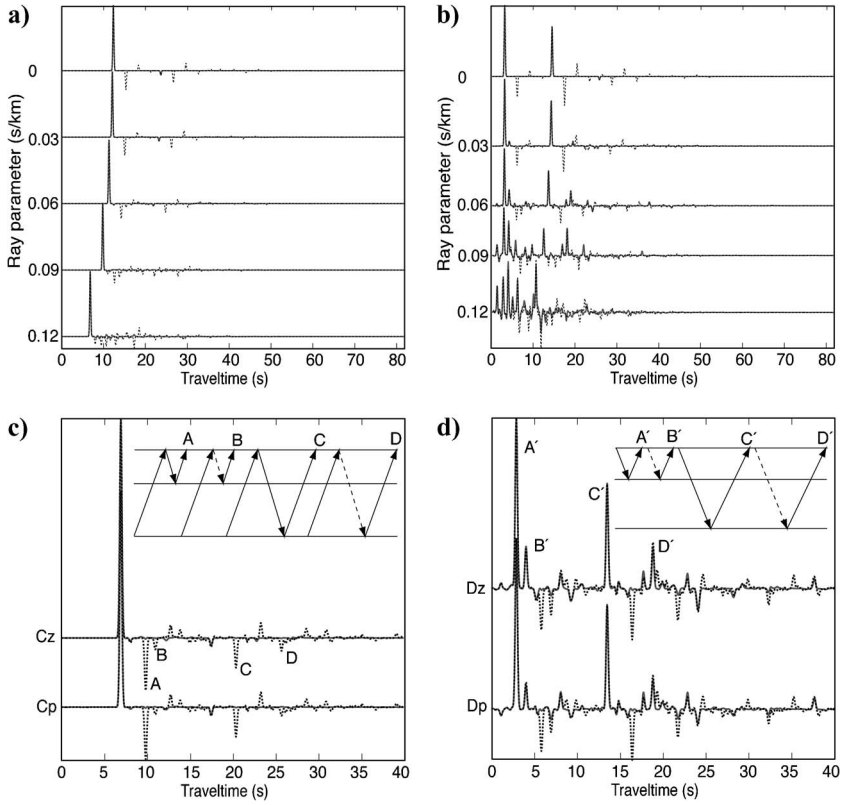

Figure 9. Elastic model simulations. For a three-layer elastic lithospheric earth model described by Table 1 at different ray parameters, (a) teleseismic responses before (dashed) and after (solid) free-surface multiple removal. The numbers on the left of each trace are the slowness (ray parameter) of the incident wavefield in s/km. (b) Reconstructed reflection responses derived from the transmission responses computed with the same model before (dashed) and after (solid) free-surface multiple removal. For ray parameter 0.06 s/km with the same model, (c) teleseismic responses of vertical (Cz) and transformed P (Cp) component before (dashed) and after (solid) free-surface multiple removal, (d) reconstructed reflection responses of vertical (Dz) and transformed P (Dp) component before (dashed) and after (solid) free-surface multiple removed. Upper case letters A, B, C, D, and A′, B′, C′, D′ indicate specific impulse responses of certain corresponding P- and converted waves. Solid arrows indicate P-waves, and dashed arrows stand for S-waves.

that will produce better estimates of P-to-SV conversion strength (receiver functions) when used to deconvolve SV and SH component data. The second element of this approach is that it provides the foundation for accurate construction of primary reflections from teleseismic P-wave data. The most commonly used approaches today cannot do this. In receiver function estimation, an operator is computed that transforms the longitudinal component data to an impulse at zero lag. This is equivalent to assuming the data recorded on the longitudinal component is not altered by any scattering in transmission through the depth range of interest (Pavlis, 2003, 2005). Baig et al. (2005) recently developed a promising alternative method to approach this problem. Their approach uses crosscorrelations between P- and SV-wavefield components and is a completely different approach to estimating the P-wave impulse response from teleseismic data.

Our expectation is that the method described in the previous sections can be applied to real data recorded station-by-station, even though the analysis is in one dimension. We base this conjecture on three things. Firstly, much current real data analysis has yielded successful results with 1D methods (e.g., Lay and Wallace, 1995): body wave modeling used for moment tensor inversion modeling, 1D receiver function, 1D waveform inversion, etc. Secondly, at the scale of teleseismic body waves (wavelength >5 km or more), the earth is dominated by vertically varying (1D) structure. This, combined with the near-vertical incidence of teleseismic body waves, suggests the approximation may not be that seriously deficient. Finally, current data give us little choice anyway. Data densities of existing teleseismic array experiments make the extension of this approach to the multidimensional form impossible. The extension to a multidimensional form may prove useful if future experiments make it applicable. The preliminary real data results by this 1D approach show promise for this method (Fan 2005; Fan and Pavlis, 2005).

CONCLUSIONS

Our method demonstrates how to remove free-surface multiples from teleseismic waves. The reflection response construction is critical for free-surface multiple removal from teleseismic wavefields. The algorithm is effective for synthetic teleseismic data with the S/N ratio higher than 5. For lower S/N ratio, the quality of the removal of free-surface multiples from transmission and constructed reflection data depends critically on the success of the construction procedure. For teleseismic wave ray parameters from 0.042 to 0.079 s/km, numerical examples show that elastic teleseismic data can be processed approximately well by the acoustic algorithm; it seems possible to process real teleseismic data with our algorithm.

ACKNOWLEDGMENTS

Support for this work came from the National Science Foundation under grants DMS-0327827 and DMS-0327778. The authors thank Robert Herrmann for his Computer Programs in Seismology software package.

REFERENCES

Backus, G., 1970, Inference from inadequate and inaccurate data: Proceedings of the National Academy of Sciences, **65**, 281–287.
Baig, A. M., M. G. Bostock and J.-P. Mercier, 2005, Spectral Reconstruction of Teleseismic-P Green's Functions: Journal of Geophysical Research, **110**, B08306.
Berkhout, A. J., 1982, Seismic migration: imaging of acoustic energy by wavefield extrapolation, A: theoretical aspects: Elsevier Scientific Publication Co.
Bostock, M., and S. Rondenay, 1999, Migration of scattered teleseismic body waves: Geophysical Journal International, **137**, 732–746.
Chapman, C. H., 1994, Reflection/transmission coefficients reciprocities in anisotropic media: Geophysical Journal International, **116**, 498–501.
Claerbout, J. F., 1968, Synthesis of a layered medium from its acoustic transmission response: Geophysics, **33**, 204–209.
——–, 1976, Fundamentals of geophysical data processing: McGraw-Hill.
de Hoop, M. V., 1992, Direct decomposition of transient acoustic wave fields: Ph.D. thesis, Delft University of Technology.
——–, 1996, Generalization of the Bremmer coupling series: Journal of Mathematical Physics, **37**, 3246–3282.
Dragoset, W. H., and Z. Jericevic, 1998, Some remarks on surface multiple attenuation: Geophysics, **63**, 772–789.
Fan, C., 2005, Extracting P-primary transmission and reflection responses from teleseismic data: Ph.D. dissertation, Indiana University.
Fan, C., and G. L. Pavlis, 2005, Extracting P-impulse responses of lithosphere from passive earthquake data: 75th Annual International Meeting, SEG, Expanded Abstracts, 1280–1283.
Fokkema, J. T., and P. M. Van Den Berg, 1993, Seismic applications of acoustic reciprocity: Elsevier Scientific Publication Co.
Frasier, C. W., 1970, Discrete time solution of plane P-SV waves in a plane layered medium: Geophysics, **35**, 197–219.
Herrmann, R. B., 2002, Computer programs in seismology, volume of An overview of synthetic seismogram computation: Saint Louis University.
Karl, J. H., 1989, An introduction to digital signal processing: Academic Press.
Kennett, B. L. N., 1991, The removal of free surface interactions from three-component seismograms: Geophysical Journal International, **104**, 153–163.
Kennett, B. L. N., N. J. Kerry, and J. H. Woodhouse, 1978, Symmetries in the reflection and transmission of elastic waves: Geophysical Journal of the Royal Astronomical Society, **52**, 215–230.
Langston, C. A., 1979, Structure under Mount Rainier, Washington, inferred from teleseismic body waves: Journal of Geophysical Research, **84**, 4749–4762.
Lay, T., and T. C. Wallace, 1995, Modern global seismology: Academic Press.
Lindenbaum, M., M. Fischer, and A. M. Bruckstein, 1994, On Gabor contribution to image enhancement: Pattern Recognition, **27**, 1–8.
Matson, K., 2000, An overview of wavelet estimation using free-surface multiple removal: The Leading Edge, **19**, 50–55.
Meyerholtz, K. A., G. L. Pavlis, and S. A. Szpakowski, 1989, Convolutional quelling in seismic tomography: Geophysics, **54**, 570–580.
Pavlis, G. L., 2003, Imaging the earth with passive seismic array: The Leading Edge, **22**, 224–231.
——–, 2005, Direct imaging of the coda of teleseismic P waves, *in* A. Levander and G. Nolet, eds., Seismic earth: Array analysis of broadband seismograms: American Geophysical Union Geophysical Monograph.
Rickett, J., and J. Claerbout, 1999, Acoustic daylight imaging via spectral factorization: Helioseismology and reservoir monitoring: The Leading Edge, **18**, 957–960.
Schuster, G. T., J. Yu, J. Sheng, and J. Rickett, 2004, Interferometric/daylight seismic imaging: Geophysical Journal International, **157**, 838–852.
Ursin, B., 1983, Review of elastic and electromagnetic wave propagation in horizontally layered media: Geophysics, **48**, 1063–1081.
Verschuur, D. J., A. J. Berkout, and C. P. A. Wapenaar, 1992, Adaptive surface-related multiple elimination: Geophysics, **57**, 1166–1177.
Vinnik, L. P., 1977, Detection of waves converted from P to SV in the mantle: Physics of the Earth and Planetary Interiors, **15**, 39–45.
Wapenaar, C. P. A., 1998, Reciprocity properties of one-way propagators: Geophysics, **63**, 1795–1798.
——–, 2003, Synthesis of an inhomogeneous medium from its acoustic transmission response: Geophysics, **68**, 1756–1759.
Wapenaar, C. P. A., D. Draganov, and J. Thorbecke, 2003, Relations between codas in reflection and transmission data and their applications in seismic imaging: 6th Society of Exploration Geophysics of Japan Annual Meeting, Expanded Abstracts, 152–159.
Wapenaar, C. P. A., and J. L. T. Grimbergen, 1996, Reciprocity theorems for one-way wave fields: Geophysical Journal International, **127**, 169–177.
Wapenaar, K., J. Thorbecke, and D. Draganov, 2004, Relations between reflection and transmission responses of three-dimensional inhomogeneous media: Geophysical Journal International, **156**, 179–194.
Weglein, A. B., F. V. Araújo, P. M. Carvalho, R. H. Stolt, K. H. Matson, R. T. Coates, D. Corrigan, D. J. Foster, S. A. Shaw, and H. Zhang, 2003, Inverse scattering series and seismic exploration: Inverse Problems, **19**, R27–R83.
Weglein, A. B., F. A. Fasparotto, P. M. Carvalho, and R. H. Stolt, 1997, An inverse scattering series method for attenuating multiples in seismic reflection data: Geophysics, **62**, 1166–1177.